

Performance Prediction Analysis of a Point Feature Tracker Based on Different Motion Models

P. Tissainayagam and D. Suter

Phone: Int+ 613 9264 3806

Fax: Int+ 613 9264 3892

[prithi, suter]@zeno.eng.monash.edu.au

Dept. of Electrical and Computer Systems Engineering

Monash University

Clayton, Victoria 3168

Australia

Abbreviated Title: **Performance of Tracking Algorithms**

Key Words: Feature tracker, Data association, Track-life, Corner extraction

Abstract

This paper provides performance prediction analysis techniques for a linear point feature tracking algorithm based on different motion models. We provide closed form expressions to evaluate the probability of correct data association of a tracker (analysed with different motion models), when tracking under clutter. We also extend our analysis for the prediction of correct data association when a tracker recovers from a false match to regain correct track. The simple mathematical expressions provided here, can be used to implement performance analysis procedures that are fast, easy, and is reasonably accurate (compared with conventional computationally expensive Monte-Carlo tracking experiments to predict the performance of a tracker). We have also demonstrated the importance of using a correct motion model for a visual tracker to get optimum tracking performance, based on empirical evaluation techniques. The performance of a tracker's robustness under varied noise has also been investigated.

Symbols Used in this Paper

$P_{ZVT}\{k+1\}$: Probability of correct association at $t=k+1$ for a ZVT

$P_{CVT}\{k+1\}$: Probability of correct association at $t=k+1$ for a CVT

$P_{CAT}\{k+1\}$: Probability of correct association at $t=k+1$ for a CAT

$P'_{ZVT}\{k+1\}$: Probability of correct association at $t=k+1$ for a ZVT, when a false match occurred at $t=k$

$P'_{CVT}\{k+1\}$: Probability of correct association at $t=k+1$ for a CVT, when a false match occurred at $t=k$

$P'_{CAT}\{k+1\}$: Probability of correct association at $t=k+1$ for a CAT, when a false match occurred at $t=k$

Performance Prediction Analysis of a Point Feature Tracker Based on Different Motion Models

1 Introduction

With the recent resurgence of interest in the area of visual tracking, many researchers are also interested in the performance of trackers for a variety of vision applications [10], [15], [19], [21]-[23], [25]-[27]. The term visual tracking, in the broader context, refers to tracking features such as corner points, lines, curves, contours, regions etc. in the image plane of a long sequence. In this paper the feature of interest is the corner points. It is important that the corner point tracker considered for a particular application be reliable when tracking in the presence of clutter, and be robust in a noisy environment. It is also equally important that the tracker in use is capable of adapting to the changing motion of features in order to provide optimum tracking results.

For the last two decades the target tracking community has been focussing on the performance of various target tracking algorithms [1]-[8], [11]. In most cases the applications of these algorithms are for specific purposes (mostly defence oriented), such as tracking missiles and satellites, to analyse aircraft manoeuvres, space-craft trajectory analysis etc. Our survey shows that in the area of image processing and pattern recognition there are very few published papers which provide performance analysis techniques for tracking algorithms for computer vision related applications. The relatively small amount of performance analysis work reported in the literature relating to visual tracking are in most cases for a narrow band of applications. They include analysing the tracking performance of a walking person [17], tracking of the left ventricle [19], evaluation of vehicle tracking [22], [26], tracking of faces [21] and body motions [18], medical diagnostics [15] etc. Most of these evaluation techniques presented are for non-point feature tracking algorithms.

Work reported in [25] use a more generalised comparison techniques to compare 4 point feature trackers. The performance of the trackers are compared only on the basis of speed of tracking algorithm in relation to the number of points tracked using a cost function strategy. In [9], [10] Ngan et. al. presented a more versatile tracker performance prediction measure called the Probability of Correct Association (PCA) for 2 trackers (a zero velocity and a constant acceleration tracker) when tracking in clutter. They also introduced the PCA concept for a tracker when recovering from a False Match (referred to as PCA-FM in this paper), but they only considered the case for the zero velocity tracker. In this paper we review their work (for completeness) and extend the performance prediction measures PCA and PCA-FM to a tracker based on the 3 different motion models (a constant acceleration,

a constant velocity and a constant position (zero velocity) models). Thus providing the extra 3 important performance measures *missing* in Ngan et. al.'s work (ie. PCA for a constant velocity model, and PCA-FM for a constant velocity and constant acceleration model). In addition, we demonstrate that the theoretical closed form performance measures are a credible representation for track results obtained by independent Monte-Carlo simulations, using real dynamic image sequences. We also empirically evaluate the performance of a complete feature tracker, the Multiple Hypothesis Tracker - MHT [14] using the different motion models considered, and we analyse its performance under varied noise levels. To emphasise the importance of choosing the correct motion model for optimal tracker performance, we also have provided results.

Since our primary task is to compare the performance of point feature trackers with different motion models, the corner features (each occupying 1 pixel in the image plane) that we track are extracted independently in each frame of a given image sequence by using the KLT corner detector [13] (It is also possible to manually label corner points of interest in each frame). By doing so we totally isolate the tracking procedure from the corner extraction procedure purely to focus on the performance of the prediction and tracking process.

The performance of a tracker is evaluated at different clutter density levels. This is achieved by artificially inserting clutter points at different densities around the actual corner features extracted (within a specified area centred at each feature). This process is employed to see whether a tracker based on a particular motion model is robust enough to associate the predicted feature point with the actual feature. Each experiment is carried out at a different clutter density level to evaluate the tracker performance.

This paper is organised as follows: Section 2 provides the assumptions that are required for the analysis. Section 3 provides the performance measures used. In section 4 and 5 the derivation of expressions for the probability of correct data association (PCA and PCA-FM) for the three trackers are considered. Section 6 outlines the experimental evaluation procedure employed. Section 7 provides the results and discussion, and finally Section 8 gives the conclusion.

2 Assumptions for Tracking Analysis

The initial objective of this paper is to develop closed form performance prediction techniques for a tracker (based on 3 linear motion models: a Zero Velocity Tracker (ZVT), a Constant Velocity Tracker (CVT) and a Constant Acceleration Tracker (CAT)). The formulation of closed form expressions for the PCA for each tracker requires a number of assumptions to be made, which are listed as follows.

Assumption 1: Only a single moving corner point is considered at a time, and the selected corner is assumed present in every frame (this is verified by a manual check following corner detection). The motion of the point feature behaves according to the following dynamic motion equations (for ZVT, CVT, and CAT respectively)

$$\mathbf{p}_k = \mathbf{p}_{k-1} + \boldsymbol{\eta}_k \quad (1)$$

$$\mathbf{p}_k = \mathbf{p}_{k-1} + \mathbf{v}_{k-1} + \boldsymbol{\eta}_k = 2\mathbf{p}_{k-1} - \mathbf{p}_{k-2} + \boldsymbol{\eta}_k \quad (2)$$

$$\mathbf{p}_k = \mathbf{p}_{k-1} + \mathbf{v}_{k-1} + \mathbf{a}_{k-1} + \boldsymbol{\eta}_k = 3\mathbf{p}_{k-1} - 3\mathbf{p}_{k-2} + \mathbf{p}_{k-3} + \boldsymbol{\eta}_k \quad (3)$$

where $\mathbf{p}_k, \mathbf{v}_k (= \mathbf{p}_k - \mathbf{p}_{k-1}), \mathbf{a}_k (= \mathbf{v}_k - \mathbf{v}_{k-1})$ are the position, velocity and acceleration at time k respectively (*per unit time*) and $\boldsymbol{\eta}_k$ is a Gaussian distributed noise.

Assumption 2: Data association is performed by the nearest neighbour method. No drift is assumed in the prediction phase when estimating the position of a feature.

Assumption 3: Clutter is present in every frame. A new set of clutter points is generated for each frame, and the clutter points are uniformly distributed in two-dimensional space for performance evaluation.

3 Performance Measures for Tracking

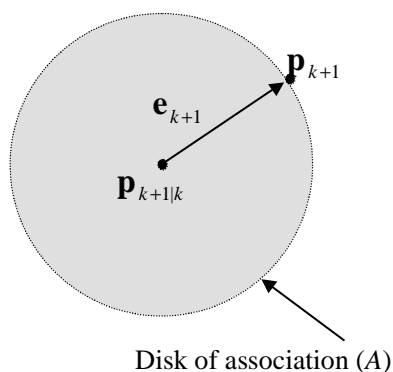


Fig. 1. Definition of prediction error.

A natural choice for a measurement of tracking performance is the *track purity* of the output trajectory generated by the tracking system. This is the average percentage of correctly associated measurements in each track, see Chang et al. [2], [3], [4]. However, an analytical expression for *track purity* is very difficult to derive. An alternative measurement is called the *Probability of Correct Association (PCA)* [10], which as its name suggests is the probability at any given step that the tracking system will make a correct data association in the presence of clutter. The following *PCA* s are presented (as performance prediction measures) in this paper.

1. The probability of obtaining the correct association at $t = k+1$ for all three trackers given that a *correct* association has been made at the *previous* time steps (referred as PCA).
2. The probability of making a correct association at $t = k+1$ for all three trackers given that an *incorrect* association has been made at $t = k$, but that a *correct* association has been made at *previous* time steps (referred as PCA-FM).

3.1 Nearest Neighbour Data Association

Denote the probability that a given pixel is not a clutter point by P_0 (and its complement by P_1), the true position of the object at $t = k+1$ by \mathbf{p}_{k+1} , and the predicted position of the object at $t = k+1$ given track positions up to and including $t = k$ by $\mathbf{p}_{k+1|k}$. Then the prediction error is defined by [10]. See Fig. 1.

$$\mathbf{e}_{k+1} = \mathbf{p}_{k+1} - \mathbf{p}_{k+1|k} \quad (4)$$

An overhead tilde is used to denote values derived from an incorrectly associated measurement made at $t = k$, thus giving rise to, $\tilde{\mathbf{p}}_{k+1|k}$, and $\tilde{\mathbf{e}}_{k+1}$.

A correct association is attained when no clutter point occurs within the region of association which is defined to be a disk with radius \mathbf{e}_{k+1} centred at $\mathbf{p}_{k+1|k}$, as shown in Fig. 1. The probability of the event of correct association is equal to the probability that no clutter point exists within a radius of \mathbf{e}_{k+1} of $\mathbf{p}_{k+1|k}$. This probability is given by the probability P_0 to the power of the number of pixels in a disk of radius \mathbf{e}_{k+1} [10], namely,

$$P\{\text{correct association at time } k+1\} = P_0^{\pi\|\mathbf{e}_{k+1}\|^2} \quad (5)$$

Thus the derivation for the probability of correct association for ZVT, CVT, CAT begins with the determination of an appropriate expression for \mathbf{e}_{k+1} for each case.

4 Probability of Correct Data Association (PCA)

This section describes the method to obtain an expression for the probability of correct association (at time step $k+1$) for each of the trackers (ZVT, CVT and CAT) assuming the tracker has not made a false match up to the current time step k .

4.1 Derivation of PCA for the Zero Velocity Tracker (ZVT)

This tracker assumes that the best prediction for the point feature in the next frame is the current point in the trajectory. Therefore, the following relationship holds for the ZVT (can also be termed the constant position tracker).

$$\mathbf{e}_{k+1} = -\mathbf{v}_{k+1} \quad (6)$$

Substituting Eq. (6) into Eq. (5) yields the expression for the probability of correct association at time step $k+1$ (denoted as $P_{ZVT}\{k+1\}$) in terms of the velocity from \mathbf{p}_k to \mathbf{p}_{k+1} . In this case the error is caused by a small velocity \mathbf{v}_{k+1} (For the ZVT, it is assumed that $\mathbf{v}_{k+1} \gg \eta_k$. Therefore, the random noise component is neglected). Therefore,

$$P_{ZVT}\{k+1 | \mathbf{v}_{k+1}\} = P_0^{\pi \|\mathbf{v}_{k+1}\|^2} \quad (7)$$

4.2 Derivation of PCA for the Constant Velocity Tracker (CVT)

The constant velocity tracker assumes correct data associations have been made at $t = k$, and $t = k-1$. The reason is that the CVT requires past positions of the feature at time k and $k-1$ to predict the position at $k+1$. If any one of these past 2 positions represent a clutter point, the calculated velocity value will not reflect the true velocity of the feature at $t = k+1$.

Using the error definition and the dynamic equations for constant velocity (section 2), we have,

$$\begin{aligned} \mathbf{e}_{k+1} &= \mathbf{p}_{k+1} - \mathbf{p}_{k+1|k} \\ &= \mathbf{p}_{k+1} - (\mathbf{p}_k + \mathbf{v}_k + \eta_k) \\ &= \mathbf{v}_{k+1} - \mathbf{v}_k + \eta_k = \mathbf{a}_{k+1} + \eta_k \end{aligned} \quad (8)$$

assume that for a non ideal case \mathbf{a}_{k+1} is non zero (say a small constant acceleration error component $\mathbf{a}_{k+1} = \mathbf{a}$ is present) and η_k is a sample from a Gaussian distributed noise. Therefore, using equations (5) and (8) the probability of correct association for CVT (denoted as $P_{CVT}\{k+1\}$) can be gives as follows:

$$P_{CVT}\{k+1 | \eta_k, \mathbf{a}_k\} = P_0^{\pi \|\mathbf{e}_{k+1}\|^2} = P_0^{\pi \|\eta_k + \mathbf{a}_k\|^2} \quad (9)$$

Using the total probability theorem [1], for the constant velocity model (CVT), we obtain,

$$P_{CVT}\{k+1 | \mathbf{a}\} = \int_{-\infty}^{+\infty} P_{v=c}\{k+1 | \eta_k, \mathbf{a}\} \cdot p(\eta_k) \cdot d\eta_k \quad (10)$$

where $p(\eta_k)$ is the pdf of the Gaussian distributed random variable η_k .

Expanding equation (10) with suitable substitution, and integrating out, produces the following expression [12]:

$$P_{CVT}\{k+1|\mathbf{a}\} = I_x \cdot I_y \quad (11)$$

where

$$I_x = \frac{e^{\gamma_x}}{4\sqrt{2\pi}\sigma_x\alpha_x^{3/2}} \left[4\alpha_x\sqrt{\pi} + 4\sqrt{\alpha_x}\beta_x + \beta_x^2\sqrt{\pi} \right]$$

with $\alpha_x = -\left(\ln P_0\pi - \frac{1}{2\sigma_x^2}\right)$, $\beta_x = 2a_x \ln P_0\pi$, $\gamma_x = a_x^2 \ln P_0\pi$. Where σ_x, a_x are the Gaussian noise variance and acceleration (\mathbf{a}) component in the x direction respectively. A similar expression can also be obtained for I_y .

4.3 Derivation of PCA for the Constant Acceleration Tracker (CAT)

Recall from section 3 that the constant acceleration tracker assumes correct data associations have been made at $t = k, k-1, k-2$. The reason for this is that the acceleration term is calculated using the previous three positions of the trajectory. If any one of these three position terms represents a clutter point, the calculated acceleration value will not reflect the true acceleration of the feature point at $t = k+1$.

The prediction error for the constant acceleration tracker is as follows (using similar approach as before).

$$\begin{aligned} \mathbf{e}_{k+1} &= \mathbf{p}_{k+1} - \mathbf{p}_{k+1|k} \\ &= \mathbf{p}_{k+1} - (\mathbf{p}_k + \mathbf{v}_k + \mathbf{a}_k + \eta_k) \\ &= \mathbf{v}_{k+1} - (\mathbf{v}_k + \mathbf{a}_k + \eta_k) = \mathbf{a}_{k+1} - (\mathbf{a}_k + \eta_k) \\ &\approx \eta_k \end{aligned} \quad (12)$$

Under the constant acceleration assumption, $\mathbf{a}_{k+1} \approx \mathbf{a}_k$ (*higher order motion terms are assumed negligible compared with the noise term, therefore not considered in (12)*). Using equation (12), the probability of correct association for CAT (denoted as $P_{CAT}\{k+1\}$) is given by;

$$P_{CAT}\{k+1|\eta_k\} = P_0^{\pi\|\eta_k\|^2} \quad (13)$$

Note that this probability is conditioned on the random component η_k , which can be integrated out by applying the *total probability theorem* as before.

The probability of correct association for CAT can be derived by setting $\mathbf{a} = 0$ in Equations (9)-(11), and simplifying the expression reduces to [12],

$$P_{CAT}\{k+1\} = \frac{1}{\sqrt{(1-2\pi\sigma_x^2 \ln P_0)(1-2\pi\sigma_y^2 \ln P_0)}} \quad (14)$$

Alternatively, the expression (14) can be obtained by expanding (13) and then simplifying using the fact that the area under a density function is unity (see [12] for a detail derivation).

5 Probability of Correct Association for Recovering from a False Match (PCA-FM)

This section describes the method to obtain an expression for the probability of correct association for each of the trackers (ZVT, CVT and CAT) when they recover from a mismatch to regain correct track (after a false match occurring in the previous time step k). An analytical derivation for ZVT is provided, but for CVT and CAT, PCA-FM expressions are provided using a combination of analytical derivation and Monte-Carlo experiments.

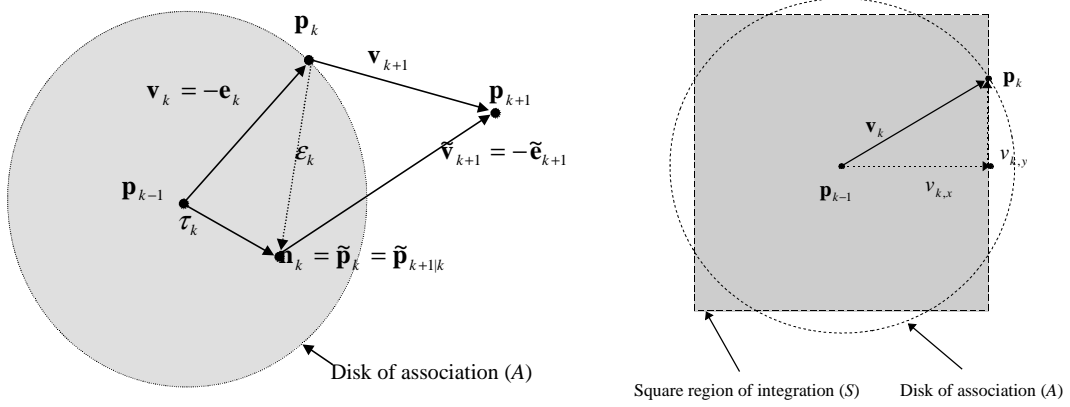


Fig. 2. Prediction error \mathbf{v}_{k+1} includes the offset due to data association error \mathcal{E}_k . **Fig. 3.** Approximating the circular region of integration A by a square region S .

5.1 Derivation of PCA-FM for the Zero Velocity Tracker (ZVT)

If a clutter point occurs within the disk shown in Fig.2 at $t = k$, then that clutter point would be selected for the trajectory at $t = k$. The probability of correct association when recovering from a false match (PCA-FM), denoted as $P'_{ZVT}\{k+1\}$, is a measure of the likelihood that the ZVT will perform a correct data association at $t = k+1$ given that an incorrect association had occurred at $t = k$. This situation is illustrated in Fig. 2.

Assume the existence of a clutter point \mathbf{n}_k inside the disk of association at time $t = k$. The nearest neighbour criterion would associate \mathbf{n}_k with the trajectory at $t = k$, which is designated the symbol $\tilde{\mathbf{p}}_k$, where the tilde denotes an incorrect association. When applying the zero velocity prediction scheme, the incorrectly associated point also

becomes the new prediction point, ie. $\tilde{\mathbf{p}}_{k+1|k} = \tilde{\mathbf{p}}_k$, and thus leading to a prediction error given by the following equation.

$$\tilde{\mathbf{e}}_{k+1} = \mathbf{p}_{k+1} - \tilde{\mathbf{p}}_{k+1|k} = \tilde{\mathbf{v}}_{k+1} \quad (15)$$

From Fig.2 it can be seen that $\tilde{\mathbf{v}}_{k+1}$ is the vector difference of the true velocity \mathbf{v}_{k+1} and the two-dimensional random variable \mathcal{E}_k as given by equation (16).

$$\tilde{\mathbf{v}}_{k+1} = \mathbf{v}_{k+1} - \mathcal{E}_k \quad (16)$$

Substituting the prediction error into equation (5) yields the probability of correct association given as follows.

$$P'_{ZVT} \{k+1 | \mathbf{v}_{k+1}, \mathcal{E}_k\} = P_0^{\pi \|\tilde{\mathbf{v}}_{k+1}\|} = P_0^{\pi \|\mathbf{v}_{k+1} - \mathcal{E}_k\|^2} \quad (17)$$

The probability $P'_{ZVT} \{k+1 | \mathbf{v}_{k+1}\}$ can be formed from equation (17) by integrating out the random term \mathcal{E}_k using the total probability theorem. The probability density function of \mathcal{E}_k is a uniform distribution inside the disk of association A , and zero outside. ie., $p(\mathcal{E}_k) = 1/\pi \|\mathbf{v}_k\|^2$ if \mathcal{E}_k is inside A , and 0 otherwise [9].

For mathematical convenience, the disk of association (A) is approximated by a square (S) as shown in Fig.3, which is centred at \mathbf{p}_{k-1} and has sides of length $2v_{\max,k}$, where $v_{\max,k}$ is defined as: $v_{\max} = \max(|v_x|, |v_y|)$.

With suitable substitution and integration, the final expression can be given by [12]:

$$P'_{ZVT} \{k+1 | \mathbf{v}\} = \frac{1}{(2v_{\max})^2} P_0^{\pi \|\mathbf{v}\|^2} I_x I_y \quad (18)$$

where, $I_x = \frac{\sqrt{\pi}}{2\sqrt{-a}} \exp\{-ab^2\} \left[\operatorname{erf}(\sqrt{-a}(v_{\max} + b)) + \operatorname{erf}(\sqrt{-a}(v_{\max} - b)) \right]$

with $a = \ln P_0 \pi$ and $b = -2v_x$. A similar expression can also be found for I_y . Note that this expression is only valid for a small velocity \mathbf{v} (to approximate a zero velocity tracker).

5.2 Derivation of PCA-FM for the Constant Acceleration Tracker (CAT)

A complete expression for the probability of correct association for a constant acceleration tracker recovering from a false match (prediction for $t = k+1$ given that at $t = k$ there is a mismatch) is rather more complicated than the zero velocity case. However, we provide a geometrical derivation using a similar vector diagram to Fig.2. An expression can be found for a *variable* disk size (instead of a fixed disk size as in Fig. 2) as shown in Fig. 4. For the ZVT it is

known that the radius of disk of association (A) is a constant velocity error ($\mathbf{e}_{k+1} = |\mathbf{v}_{k+1}|$). But for a CAT we model the radius r (with components r_x, r_y in the x, y direction) of A as a variable quantity.

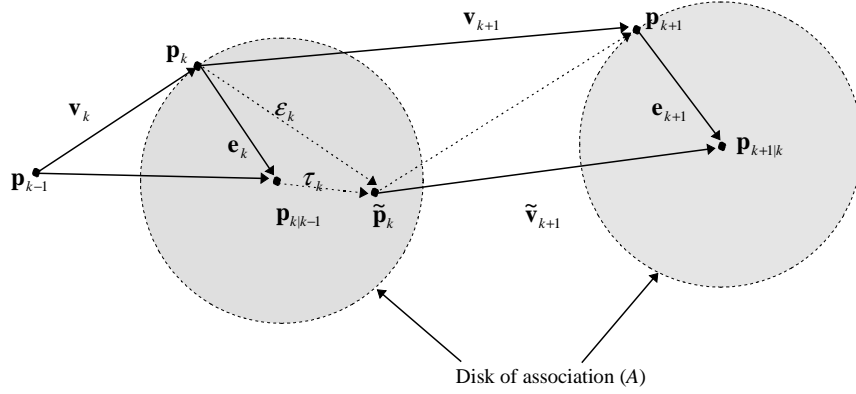


Fig.4. Vector diagram for the probability of correct association for CAT and CVT when recovering from a mismatch (the radius of the disk of association is modelled as a variable quantity).

From vector diagram (Fig. 4), and with the motion equation for CAT it can be shown (with assumptions (i), (ii) given below) that:

$$\mathbf{e}_{k+1} \approx (r + \tau_k)/2 \quad (19)$$

where \mathbf{e}_k ($= r$) is the radius of the disk of association (the error) for the matching at $t = k$.

Assumptions for deriving (19):

- (i) τ_k is a random error term (non Gaussian) between the actual position of the feature and the selected mismatched feature (at $t = k$).
- (ii) $\tau_k \gg \eta_k$ (for low noise levels).

By a similar analysis as to that carried out for the ZVT, the probability of correct association for PCA-FM (recovering from a false match), denoted as $P'_{CAT}\{k+1|r\}$, can be given by (See [12] for details):

$$P'_{CAT}\{k+1|r\} = \frac{1}{4r_{\max}^2} P_0^{\frac{\pi}{4} r_{\max}^2} I_x I_y \quad (20)$$

where $2r_{\max}$ is the length of the square (whose area approximates that of the circle, as for the ZVT case) and

$r_{\max} = \max(|r_x|, |r_y|)$. The I_x is given by,

$$I_x = \frac{\sqrt{\pi}}{2\sqrt{a}} \exp\{ar_x^2\} \left[\operatorname{erf}(\sqrt{a}(r_{\max} + r_x)) + \operatorname{erf}(\sqrt{a}(r_{\max} - r_x)) \right]$$

with $a = -\ln P_0 \frac{\pi}{4}$ and r_x is the x component of r , and can be given by the following expression [12]:

$$\begin{aligned} r_x &= [\alpha + \beta \exp\{-(bh^2 + ch + d)\}] \cdot h_x \\ &= f(h_x, h_y) \cdot h_x \end{aligned} \quad (21)$$

where h is an error quantity (a higher order motion, considered as an error term) of the dynamic system (h_x is the x component of h), and α, β, b, c, d are constants. The expression for r_x was evaluated by performing extensive Monte-Carlo simulations (a mathematical closed form expression for r_x is very difficult to derive). The following approximate values for the constants were also obtained by Monte-Carlo methods; $\alpha = 2, \beta = 28, b = 1.5, c = 2, d = 0.03$ for CAT. A similar expression to Eq. (21) can be given for I_y and r_y .

Equation (20) is very similar to equation (18) except that r is a *variable size* in this case. Through a series of Monte Carlo simulations, using a range of modelled error terms (such as the rate of change of acceleration) and disk radius values (r), we were able to create close matches between the experimental probability of correct association (PCA-FM) and the theoretical expression given in equation (20). The result of these experiments is given in the plot in Fig.5. This shows the variation of $f(h_x, h_y)$ with h . A perfect CAT is obtained when $h \rightarrow 0$. Conversely, with the use of this plot for a given error term (eg: acceleration of acceleration) we can find r (using equation 21), and in turn be able to find the probability of correct data association using Equation (20).

5.3 Derivation of PCA-FM for the Constant Velocity Tracker (CVT)

For the derivation of PCA-FM for CVT (denoted as $P'_{CVT} \{k+1 | r\}$), a similar analysis can be carried out as for the CAT. In this case a constant velocity model is assumed with a constant acceleration error term added to the dynamic motion equation. The probability of correct association (recovering from a mismatch) is still given by equation (20), but r_x is now given by the following expression.

$$\begin{aligned} r_x &= [\alpha + \beta \exp\{-(bg + c)\}] \cdot g_x \\ &= f(g_x, g_y) \cdot g_x \end{aligned} \quad (22)$$

where g is the acceleration (modelled error term) of the dynamic system (g_x is the x component of g), and α, β, b, c are constants (as before) and were found to be approximately: $\alpha = 2.2, \beta = 18, b = 2.5, c = 0.03$ through a series of simulations. The variation of $f(g_x, g_y)$ with g is shown in Fig. 6. As before a perfect CVT is obtained when $g \rightarrow 0$.

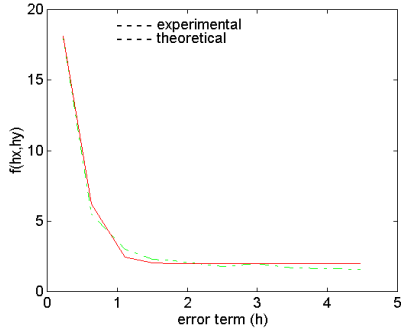


Fig. 5

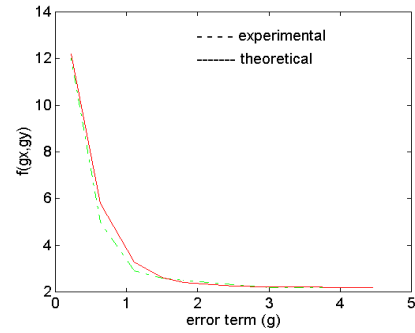


Fig. 6

Fig. 5. Variation of $f(h_x, h_y)$ with the error term (h). As $h \rightarrow 0$ a perfect CAT model is obtained. **Fig. 6.** Variation of $f(g_x, g_y)$ with the error term (g). As $g \rightarrow 0$, a perfect CVT model is obtained.

6 Experimental Procedure

This section describes the experimental procedure used to empirically validate the probabilities of correct association (for complete experimental process the reader is referred to [12]).

6.1 Generation of Clutter Points

For each frame of a sequence, a set of random tokens is added to represent clutter. The random tokens are uniformly distributed in each frame using a specified clutter density P_1 (see section 3.1 for definition of P_1). The spatial region over which the new tokens are deposited is centred at the reference corner point and is a square region with a sufficient number of pixels so that the expected number of deposited (within the region) clutter tokens is N . In the experiments N was set to 10. The value of N cannot be set too high because the extent of the clutter region grows very large with small values of P_1 . Having N large can be computationally impractical in the current implementation. The set of P_1 values used, were (0.0001 0.0002 0.0005 0.001 0.002 0.005 0.01 0.02 0.05 0.1 0.156 0.277 0.625). These are the 13 clutter levels at which the probability of correct association is evaluated.

6.2 Calculation of Probability of Correct Association

The probabilities of correct association (PCA and PCA-FM) for simulations are calculated using the following expressions for each tracker (where event types A , B , C , and D are defined below):

$$P_{ZVT}\{k+1; \mathbf{v}_{k+1}\}, P_{CVT}\{k+1\}, P_{CAT}\{k+1\} = \frac{A}{A+B}$$

$$P'_{ZVT}\{k+1; \mathbf{v}_{k+1}\}, P'_{CVT}\{k+1\}, P'_{CAT}\{k+1\} = \frac{C}{C+D}$$

Type A: Indicates correct tracking at time k ; **Type B:** Incorrect tracking at time k ; **Type C:** Indicates recovery from incorrect tracking at time k ; **Type D:** Continuation of error due to incorrect tracking at time k .

7 Results

The following sub-sections describe the qualitative and quantitative results obtained for the various empirical evaluations presented. The simulated tracking performance is evaluated under 2 categories. The *track life* (Total number of correct trajectory points regardless of trajectory order) and *track purity* (Number of frames to first incorrect trajectory point). Our analysis as discussed below shows that the PCA and PCA-FM derived (for each separate motion model) are a good representation for the simulated *track life* and *track purity*, respectively, for each image sequence considered. All our experiments presented here are based on real life dynamic image sequences. Finally, we employ a complete feature tracker (The Multiple Hypothesis Tracker [14] is chosen for demonstration) and show the quality of feature trajectories obtained using different motion models described. The experiments are also carried out at varied noise levels to test the robustness of the tracker.

7.1 Track Life and Track Purity Results Under Clutter

The results presented in Figs. (7-12) shows that the closed form expressions (PCA and PCA-FM) are a reasonable match to the Monte Carlo experiments (using synthetic data), provided there is no violation of assumptions made in deriving the theoretical expressions (as given in sections 4 and 5). This suggests that the theoretical expressions are a credible representation of tracker performance (for each separate motion model) under varied clutter level. For each experiment more than 100 separate Monte Carlo runs were made and the average considered.

The trackers (ZVT, CVT, CAT) were applied to track corner features (extracted independently of the tracker, using the KLT corner detection algorithms [13]) for image sequences ranging from about 10 to 50 frames. We used a variety of different image sequences with the feature to be tracked moving with varied motion (due either to feature motion or camera motion). Figures 13-16 and 17-20 shows the track life and track purity results for the PUMA (30 frames), Toy-Car (9 frames), Walking-Man (50 frames) and RUBIC (20 frames) image sequences respectively. From these results it is reasonably clear that a CAT or a CVT tracker gives the best tracking results for

the PUMA sequence, while a CVT seems more suitable for the Walking man and Toy car sequences. A ZVT is adequate for the RUBIC sequence, this is because the inter-frame motion for the RUBIC sequence is very small, thus a zero velocity tracker is able to produce trajectories which are comparable to CVT and CAT. The same results are independently verified by visually inspecting the qualitative results given in Figs. 21 (these tracks are obtained by using the MHT employing the 3 different motion models discussed). The motion model that gives the best quality trajectories (for each image sequence) is the same as the ones revealed by Fig. 13-16 and Figs.17-20, thus confirming the consistency of the results presented.

7.2 Application of MHT Employing Different Motion Model in the Presence of Noise

The MHT tracker with the most suitable motion model as applicable to each of the image sequence considered (obtained from results reported in sections 7.1) was tested under noisy condition. The noise (uncorrelated noise) is artificially added to each frame (except the first frame) of a sequence at a specified noise variance. The process was followed by feature extraction prior to applying the tracker. Figures 22 shows the qualitative tracking results of MHT under varied noise levels. For this series of experiments the number of features extracted in the initial frame for each sequence was limited to around 25 for clarity. The results (Fig. 23) are similar to tracking in clutter, this is because the false corner points detected by the corner-extracting algorithm are treated like cutter by the tracker.

7.3 Theoretical Results versus Experimental Results

From the plots given in Figures 7–20, it is clear that there is deviation between the theoretical and experimental (simulation) results. The reasons for the deviation could be attributed to the following.

- (a) In deriving the theoretical expressions, many assumptions were made (as described in sections 4.1-4.3 and 5.1-5.3). These were necessary in order to obtain feasible mathematical formulations. Whereas the simulated experiments were all based on the true dynamic motion models. Failure to meet these assumptions could have caused discrepancy.
- (b) Obtaining PCA and PCA-FM using simulations were based on several hundreds of Monte Carlo runs (100-300). The number of runs might not have been sufficient for true representation of event types *A*, *B*, *C* and *D*. Particularly, the conditions required for event types *C* and *D* are rather restricted and thus the probabilities of events *C* and *D* occurring is very low, which in turn could have led to the calculation of less reliable probability values. This could have caused some deviation between the theoretical and simulated results.

(c) Numerical approximation and compromises in simulation implementation methods could have caused some deviation, which were not accounted for in the analytical study.

However, despite these factors, the correspondence between the theoretical formulation and experimental results are close for low and high values of clutter density.

8 Conclusion

We have provided a performance prediction scheme for simple linear trackers based on different motion models when tracking under clutter. The closed form expressions provided for performance prediction have been shown to be more efficient than the conventional Monte-Carlo experiments. The method provided is useful to compare the performances of a visual tracker based on different motion models, thus indicating to the model that gives the best quality trajectories. We have also experimentally demonstrated that choosing the most appropriate motion model is important for any tracker to provide good tracking results. The tracker performance under noise has also revealed some interesting results. This was demonstrated by applying the MHT tracker to track features at varied noise levels.

In another line of research we carried out, we proposed a multiple motion model tracking algorithm [23] which was capable of automatically switching to the most suitable motion model presented (from a bank of motion models) that best described the feature's motion, resulting in good feature trajectories. The algorithm utilised the Interacting Motion Model (IMM) [1] criteria for model switching. The image sequences used in [23] were the same as the ones used in this paper, and the outcome of the optimal model selection revealed in [23] matches the results presented here, thus confirming the consistency of motion model selection results for each sequence considered.

References

1. Y. Bar-Shalom and X. R. Li, *Estimation and Tracking: Principles, Techniques, and Software*, Artech House, MA, 1993.
2. K. C. Chang, "Multitarget tracking with adaptive detection thresholds", *IEEE Trans. on Aerospace and Electronic Systems*, Vol.32, No.1, pp.401-406, 1996.
3. K. C. Chang, S. Mori, and C. Y. Chong, "Evaluating a Multiple Hypothesis Multitarget Tracking Algorithm", *IEEE Trans. on Aerospace and Electronic Systems*, Vol.30, No.2, April 1994.
4. K. C. Chang, S. Mori, and C. Y. Chong, "Performance evaluation of track initiation in dense target environments", *IEEE Trans. on Aerospace and Electronic Systems*, Vol.30, No.1, Jan. 1994.
5. X. R. Li and Y. Bar-Shalom, "Detection threshold selection for tracking performance optimization", *IEEE Trans. on Aerospace and Electronic Systems*, Vol.30, No.3, July 1994.

6. X. R. Li and Y. Bar-Shalom, "Performance prediction of tracking in clutter with nearest neighbour filters", *Proceedings of the SPIE*, Vol. 2235, pp.429-440, 1994.
7. X. R. Li and Y. Bar-Shalom, "Performance prediction of the Interacting Multiple Model Algorithm", *IEEE Trans. on Aerospace and Electronic Systems*, Vol.29, No.3, July 1993.
8. S. Mori, K. C. Chang, and C. Y. Chong, "Performance Analysis of Optimal Data Association - with applications to multiple target tracking", in *Multitarget-Multisensor Tracking: Applications and Advances. Vol. II*, Artech House, 1992.
9. P. M. Ngan, "Image sequence analysis 1995-96", *Tech. Report 571*, Industrial Research Limited, Auckland, New Zealand, June 1996.
10. P. M. Ngan and A. M. McIvor, "Performance Analysis of Two Tracking Methods", In *Image and Vision Computing New Zealand 1995*.
11. S. R. Rogers, "Diffusion analysis of track loss in clutter", *IEEE Trans. on Aerospace and Electronic Systems*, 27(2): pp.380-387, March 1991.
12. P. Tissainayagam and D. Suter, "Performance Analysis of Point Feature Trackers", *Technical report MECSE-1998-6*, Monash University, Australia. 1998.
13. C. Tomasi and T. Kanade, "Detection and Tracking of Point Features", Carnegie Mellon University, Tech. Report CMU-CS-91-132, April 1991.
14. I. J. Cox and S. L. Hingorani, "An Efficient Implementation of Reid's Multiple Hypothesis Tracking Algorithm and Its Evaluation for the Purpose of Visual Tracking", *IEEE Trans. on PAMI*, vol.18, no.2, Feb. 1996.
15. A. Blake and M. Isard, *Active Contours*, Springer Verlag, 1998.
16. P. Tissainayagam and D. Suter, "Performance Prediction Analysis of Visual Tracking Algorithms", In *proc. Irish Machine Vision Conference '99*
17. A. M. Baumberg and D. Hogg, "An efficient method for contour tracking using active shape models", In *Proc. of the IEEE Workshop on Motion of Non-Rigid and Articulate Objects*, pp.194-199, 1994.
18. A. Blake, M. Isard and D. Reynard, "Learning to track the visual motion of contours", *AI*, 78, pp.101-134, 1995.
19. A. Blake and A. Yuille (editors), *Active Vision*, MIT press, 1992.
21. T. F. Cootes, C. J. Taylor, A. Lantis, D. H. Cooper, and J. Graham, "Building and using flexible models incorporating grey-level information. In *Proc. ICCV'93*, pp.242-246, 1993.
22. D. Koller, J. Weber and J. Malik, "Robust multiple car tracking with occlusion reasoning", *ECCV'94*, pp.189-196.
23. P. Tissainayagam and D. Suter, "Visual Tracking and Motion Determination using the IMM Algorithm", *ICPR '98*, pp.289-291, 1998.
25. J. Verestoy and D. Chetverikov, "Experimental Comparative Evaluation of Feature Point Tracking Algorithms", *Evaluation and Validation of Computer Vision Algorithms*, Kluwer Series in Computational Imaging and Vision, 2000, pp.183-194.
26. K. D. Baker and G. D. Sullivan, "Performance assessment of model based tracking", *Workshop on Applications of Computer Vision*, pp.28-35, 1992

Theoretical versus experimental results (using synthetic data)

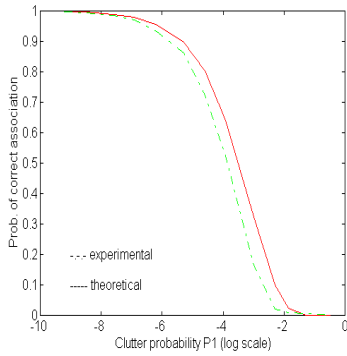


Fig. 7

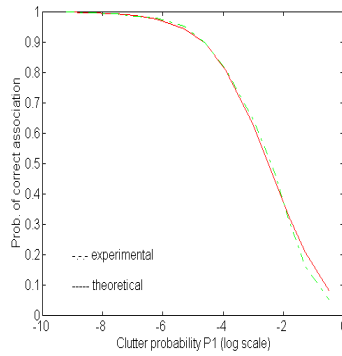


Fig. 8

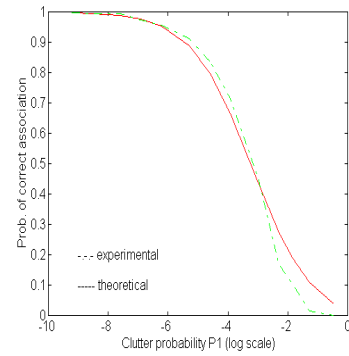


Fig. 9

Fig. 7. Probability of correct association for the ZVT. P_1 is shown on a log scale. A velocity error (v) of 6.25 pixels/unit time was modelled as an error term for the ZVT tracker. **Fig. 8.** Probability of correct association for the CVT. The Gaussian noise variance $\sigma=1.3$ with an added acceleration error of 0.01 pixels/unit time/unit time (modelled as an error). **Fig. 9.** Probability of correct association for the CAT. The Noise variance is set to $\sigma=1.3$.

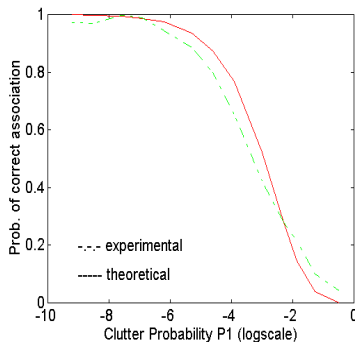


Fig. 10

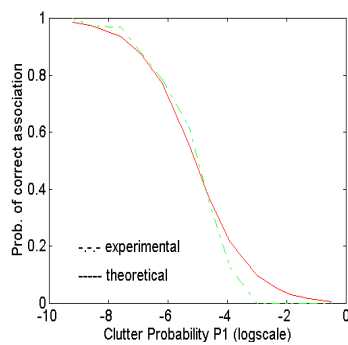


Fig. 11

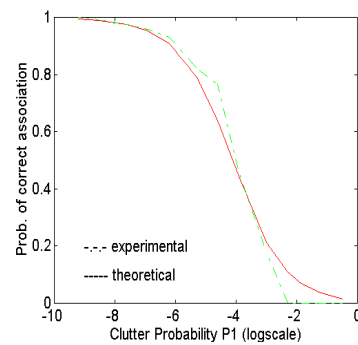


Fig. 12

Fig.10. Probability of correct association for the ZVT case for recovering from a mismatch. P_1 is shown on a log scale. The velocity error ($v=1.0$ pixels/unit time). **Fig.11.** Probability of correct association for the CVT, case for recovering from a mismatch. The variable disk of association radius $r = 4.4$, with $f(g_x, g_y) = 2.2$. **Fig.12.** Probability of correct association for the CAT for recovering from a mismatch. Acceleration error (In this case the variable disk of association $r = 2.9$, with $f(h_x, h_y) = 2$).

Track-life results (using real data)

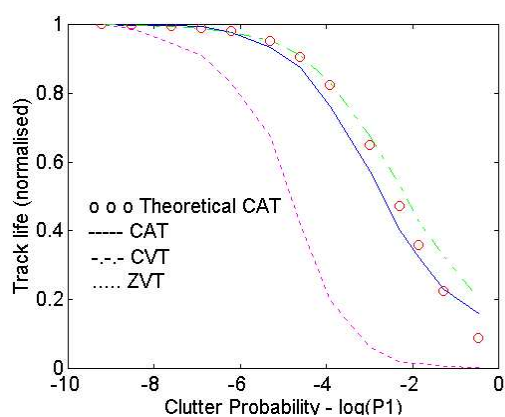


Fig. 13

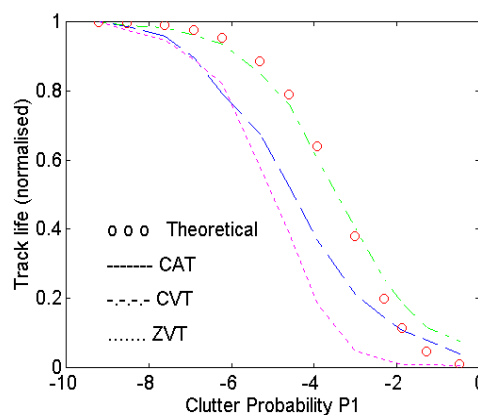


Fig. 14

Fig. 13. Track-life for the PUMA sequence plotted against clutter probability (shown in log scale). The theoretical model presented for the probability of correct association (for CAT) closely matches the track life obtained using a constant acceleration tracker (CAT) experimentally. The plot shows that a CAT or CVT provides the best quality trajectories under clutter for the PUMA sequence. **Fig. 14.** Track-life for Walking man sequence. The track-life obtained by experiments for walking man sequence using a constant velocity model (CVT) gives the best match for the theoretical CVT model.

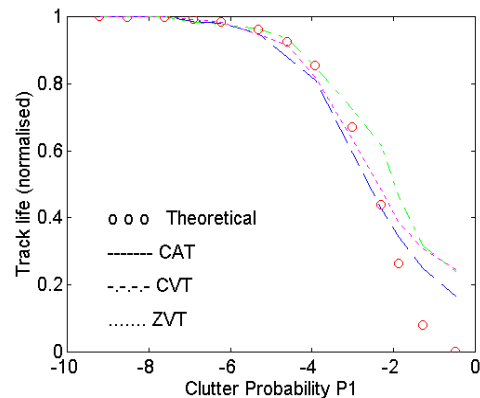


Fig. 15

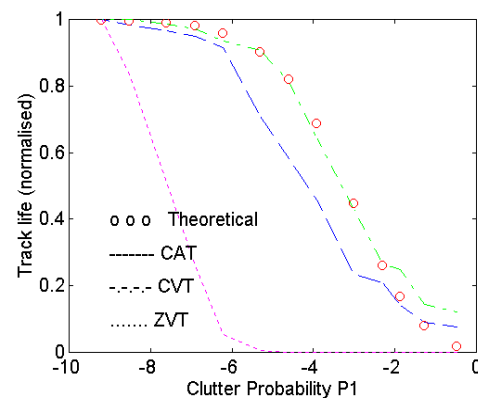


Fig. 16

Fig. 15. Track-life for the RUBIC sequence plotted against clutter probability (shown in log scale). The theoretical model presented for the probability of correct association (for ZVT) matches track-life obtained by all 3 trackers. Since the motion is very small between frames, a ZVT tracker seems adequate.

Fig. 16. Track-life for Toy car sequence. The track-life obtained for toy car sequence using a constant velocity model (CVT) gives the best match for the theoretical CVT model presented.

Track-purity results (using real data)

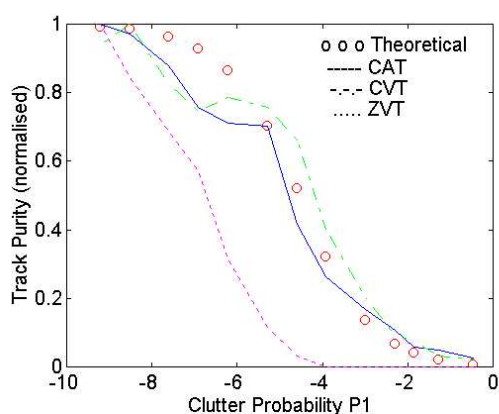


Fig. 17

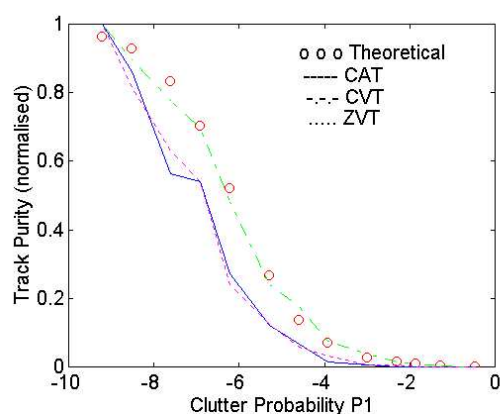


Fig. 18

Fig. 17. Track-purity for the PUMA sequence plotted against clutter probability (shown in log scale). The theoretical model presented for the probability of correct association for recovering from a mismatch (for CAT) is a reasonable approximation to the track-purity obtained using a constant acceleration tracker (CAT) by simulations. This is an indication that for feature tracking for the PUMA sequence a CAT or CVT provides the best track result.

Fig. 18. Track-purity for Walking man sequence. The track-purity obtained for walking man sequence (by simulations) using a constant velocity model (CVT) gives the best match for the theoretical CVT model.

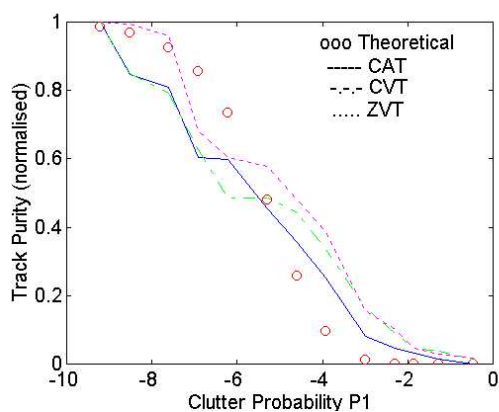


Fig. 19

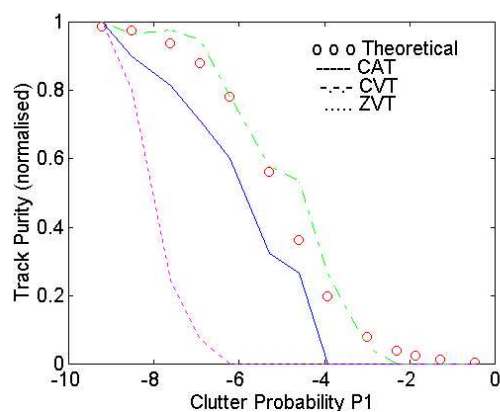


Fig. 20

Fig. 19. Track-purity for the RUBIC sequence plotted against clutter probability (shown in log scale). The theoretical model presented for the probability of correct association (for ZVT) when recovering from a mismatch is a reasonable match for tracks obtained by all 3 trackers (using simulations). Since the motion is very small between frames, a ZVT tracker is adequate.

Fig. 20. Track-purity for Toy car sequence. The track-purity obtained (by simulations) for toy car sequence using a constant velocity model (CVT) is reasonably a good match for the theoretical CVT model presented.